

MMC has three objectives. First objective and second objective are the input current control and the output voltage control. The input current control and the output voltage control have the same requirement to the conventional AC-DC converters which applies the MMC. For example, the control strategies for the AC-DC converters which applies the MMC have been proposed⁽¹⁴⁾⁻⁽¹⁶⁾. The control system has three current control systems in order to control independently the DC circulating current, the AC circulating current and the input or output AC current which flows to the utility grid. Besides, the control system has two voltage control systems in order to control the average voltage in the cell capacitors and correct an unbalance voltage among the cells. Thus, there are many control parameters. However, the design method for the parameters in each control system has not been reported⁽¹⁴⁾. On the other hand, an analysis based on an equivalent circuit of the MMC and other control strategy has been reported⁽¹⁵⁾. However, there are also many control parameters which should be designed. Similarly, the modeling of the MMC and the control strategy which is based on the equivalent circuit have been proposed⁽¹⁶⁾. Specifically, the control methods of the negative sequence current and the zero sequence current in the unbalance of the utility grid have been proposed. However, it seems that the detail of the voltage control for the capacitors has not been described. Moreover, the control scheme which is included the voltage control for the capacitors has not also been shown.

Third objective is the capacitor balancing control in each cell. It is important to balance the capacitor voltage in each cell at constant because the circuit devices may be broken in a worst-case when the unbalance of the charge voltage in each cell occurs. The control method in order to balance the capacitor voltage have been reported^{(8), (18)-(19)}. However, it seems that the design method for the control parameters of the capacitor voltage balancing control has not discussed. Additionally, it is also necessary to determine the sign of the arm current in the conventional control⁽⁸⁾. Moreover, other control methods have been proposed in the condition at the low switching frequency. However, the unbalance voltages among all cells are not eliminated completely⁽¹⁸⁾⁻⁽¹⁹⁾.

This paper proposes the control strategy of the MMC based on the control strategy for the single-phase power factor correction (PFC) converter with an aim to apply the conventional control techniques of the PFC converter to the MMC. In particular, the main parts of the current control for the input AC current and the voltage control for the capacitor voltage are constructed by the control strategy of the single-phase PFC converter. The key idea is that the H-bridge cell has same circuit configuration as single-phase PFC converter. Moreover, the PFC converter and the H-bridge cell have many common points in the circuit operation and the control strategy. For example, the capacitor voltage is required to be maintained at constant in both circuits. Furthermore, it is necessary to control the input AC current in order to maintain the capacitor voltage and reduce the total harmonic distortion (THD). In addition, the control strategy, the design method for control parameters and the stability analysis of the control system for PFC converters have been considered so far⁽¹⁹⁾⁻⁽²²⁾. As a conclusion, the control techniques can be applied to the control system for the MMC without major modification of the control strategy if the MMC is able to be controlled by the proposed control strategies based on the control strategy for the PFC converter. Moreover, it is expected that it is possible to propose new ideas and new points of view for a control method of the MMC by applying control technologies of the

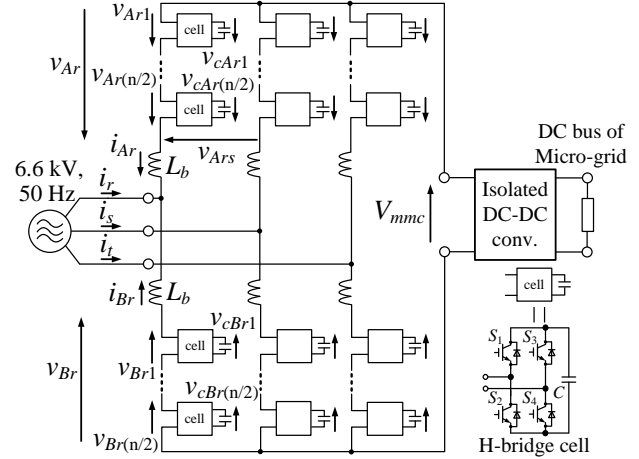


Fig. 1. Circuit configuration of step-down rectifier which applies MMC for DC Micro-grid. The MMC with H-bridge cells operates as a step-down rectifier.

single-phase PFC converters. However, it seems that the employment of the control strategy for the PFC converter into the MMC has considered scarcely.

In addition, the control method in order to balance the capacitor voltages in all cells is also proposed. The main advantage of the proposed capacitor voltage balancing control is that it is not necessary to design the control parameters because the dividing ratio is adjusted automatically depending on the capacitor voltage. Moreover, it is not also necessary to determine the sign of the arm current in the proposed voltage balancing control.

This paper is organized as follows. First, in section 2, the circuit configuration of the step-down rectifier which applies the MMC with H-bridge cells are shown. The relationship between the circuit configuration of the cell and its output voltage are demonstrated. In section 3, the control system based on the control strategy of the single-phase PFC converter is proposed. Additionally, the principle of the proposed capacitor voltage balancing control is also explained. In section 5, the simulation result of the MMC which employs the proposed control strategy is shown. Finally, in section 6, the experimental results of a miniature model in the utility grid of 200 V are shown.

2. Circuit Configuration

2.1 Main Circuit Configuration Fig. 1 shows a main circuit configuration of the step-down rectifier which applies the MMC for DC Micro-grids. The proposed system converts from a medium voltage of an input power grid to a DC bus voltage of the DC Micro-grid.

First, the step-down rectifier which applies the MMC converts from the medium voltage of 6.6 kV to the DC voltage of several hundred volts. Each arm of the MMC consists of a buffer inductor L_b and cascade connected cells. As features of the multilevel converter, the proposed converter which applies the MMC outputs a multi-level voltage waveform which is changed by the number of cascade connected cells. Additionally, low voltage rating devices are applied to each cell because the proposed step-down rectifier reduces the voltage dividing value of each cell by increasing the number of cascade cells. Thus, the number of cascaded cells is increased in practical in order to reduce harmonic distortion and utilize low voltage rating devices.

Second, a high power isolated DC-DC converter supplies the DC bus voltage of 400 V. In the proposed system shown in Fig. 1, a dual active bridge (DAB) converter is considered to be suitable to be applied as a high power isolated DC-DC converter⁽²³⁾⁻⁽²⁵⁾. The proposed system requires a DC-DC converter for the bidirectional operation and the isolation with high efficiency and small volume. The DAB converter can achieve the bidirectional operation with high efficiency by using zero voltage switching (ZVS). Moreover, the DAB converter also achieves the isolation between the utility grid and the DC micro-grid with the small high frequency transformer. Thus, it is possible to reduce the volume of the system because of the utilization of the high frequency transformer.

On the other hand, in the MMC, the output DC voltage depends on the summation of the average value of cell output voltage. Generally, many AC-DC converters which apply the MMC are constructed by chopper cells⁽¹⁴⁾. However, conventional AC-DC converters which apply the MMC with chopper cells cannot achieve step-down rectification because the limit of the average value of cell output voltage exists in the chopper cell. In contrast, the H-bridge cell has no limit of the average value of cell output voltage because the H-bridge cell can output a negative voltage. Therefore, it is able for the H-bridge cell to vary the average value of the cell output voltage. Thus, the MMC which is consisted of H-bridge cells achieves step-down rectification. Note that the upper arm group and the lower arm group are defined A and B respectively.

At first, the step-down rectifier which applies the MMC is required to achieve both the input current control and the output DC voltage control. Therefore, the output voltage of each cell on one leg and the capacitor voltage are depended by the maximum value of the input phase voltage, the output DC voltage and the number of cells on one leg. The capacitor voltage command v_c^* is given by (1). Note that the voltage drop of the buffer inductor is ignored because the voltage drop is sufficiently small compared to voltages of the input side and the output side.

$$v_c^* \geq \frac{1}{n\lambda} \left(2\sqrt{\frac{2}{3}}E + V_{mmc}^* \right) \dots\dots\dots (1)$$

where E is the effective value of the input line-to-line voltage, V_{mmc}^* is the command of the output DC voltage of the MMC, n is the number of cells at each leg, λ is a modulation index.

Table 1 shows configuration examples of switching devices and cell capacitors which are necessary to construct the MMC when the MMC is applied into the DC Micro-grid as the step-down rectifier. The power capacity of the system is 300 kW⁽³⁾⁻⁽⁴⁾. Moreover, the medium voltage grid of 6.6 kV is applied as the input voltage source. On the other hand, the DC voltage of the Micro-grid is 400 V⁽⁴⁾⁻⁽⁵⁾. In table 1, the capacitor voltage is calculated by (1) when the modulation index λ is set to 0.9. Additionally, the voltage rating of the IGBT is set twice more than the capacitor voltage. The current rating of IGBT is set 70% more than the each arm current. From the above condition, the voltage rating of the IGBT is 3300 V and the current rating is 400 A. Examples of high power IGBTs which meet the conditions of the voltage rating and the current rating are shown.

2.2 Relationship between Cell Circuit Configurations and Output Voltage

Fig. 2 shows relationships between circuit configurations of cells and cell output voltages. In the AC-DC converter which applies the MMC, the maximum value of the input phase voltage is applied to each arm when the AC-DC converter operates. Hence, the peak-to-peak value of the cell voltage v_{cell_p-p} is given by (2) from the input phase voltage and the number of cells

Table 1. Configuration example of MMC for DC micro-grid system @300 kW

Voltage rating of IGBT	3300 V
Current rating of IGBT	400 A
Capacitor voltage @ $\lambda = 0.9$	1500 V
Numbers of Cells @ leg	8
Total numbers of Cells	24
Numbers of Switching Device	96
Examples of IGBTs ⁽²⁶⁾⁻⁽²⁸⁾	MBM400E33D-MFR (Hitachi, Ltd.) FZ400R33KL2C_B9 (Infineon) 5SLG 0500P330300 (ABB)

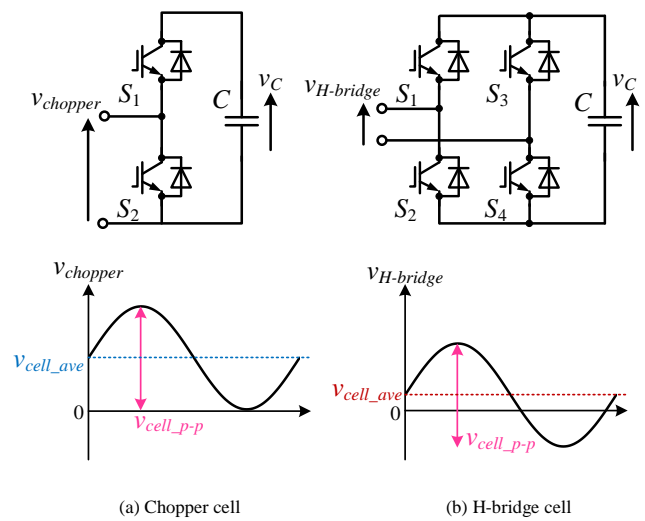


Fig. 2. Relationship between circuit configuration and output voltage of each cell. The chopper cell has the lower limit of the output voltage because the chopper cell cannot output the negative voltage. On the other hand, the H-bridge cell has no lower limit of the output voltage per leg.

$$v_{cell_p-p} = 4\sqrt{\frac{2}{3}} \frac{E}{n} \dots\dots\dots (2)$$

In addition, the output DC voltage of the MMC V_{mmc} equals the summation of average values of the cell output voltages at one leg. Hence, V_{mmc} is given by (3). Note that all average values of the cell output voltages are same.

$$V_{mmc} = nv_{cell_ave} \dots\dots\dots (3)$$

where v_{cell_ave} is the average value of the cell output voltage.

Fig. 2(a) shows the relationship between the chopper cell and its output voltage. In the case of applying the chopper cell to the MMC, a lower limit of the average output voltage is uniquely determined from the peak-to-peak value of the cell voltage v_{cell_p-p} and the number of cells at each leg n because the chopper cell cannot output the negative voltage. Therefore, the chopper cell has the lower limit of the average output voltage. The lower limit of the average output voltage $v_{cell_ave_LL}$ is given by (4) based on Fig. 2(a).

$$v_{cell_ave_LL} = \frac{1}{2} v_{cell_p-p} \dots\dots\dots (4)$$

From (2), (3) and (4), the lower limit of the output DC voltage of the MMC V_{mmc} equals twice the value of the maximum voltage of the input phase voltage. From the principle of the above, the MMC with chopper cells cannot achieve step-down rectification.

Fig. 2(b) shows the relationship between the circuit configuration of the H-bridge cell and its output voltage. In the case of the H-bridge cell, there is no limit of average value of the cell output voltage because it is possible for the H-bridge cell to output the negative voltage. Hence, it is possible for H-bridge cell to control lower voltage than that of (4). Therefore, the MMC with H-bridge cells achieves step-down rectification.

3. Proposed Control Strategy

Fig. 3 shows the control block diagram of the proposed step-down rectifier which applies the MMC. As one of the features of the proposed control, each arm as shown in Fig. 1 is individually controlled. The proposed control is based on the single-phase PFC converter because the H-bridge cell has same circuit configuration as single-phase PFC converter. Moreover, the PFC converter and the H-bridge cell have many common points in the circuit operation and the control. For example, the capacitor voltage is required to be maintained constant in both circuits. Moreover, it is necessary to control the input AC current in order to maintain the capacitor voltage and reduce the total harmonic distortion (THD). Differences between the PFC converters and the H-bridge cells are; there is the DC component in the output voltage of the H-bridge cell, and a capacitor voltage balancing control is necessary in order to correct the unbalance voltages among all capacitors. Thus, in order to deal with above problems, it is necessary to add two controls in order to control the DC component and achieve the capacitor voltage balancing into the conventional control of the PFC converters.

In particular, in order to control each arm, the control block diagram is separated to the capacitor voltage control block and the input current control (Automatic Current Regulator: ACR) block. Moreover, the capacitor voltage control block consists of a capacitor voltage averaging control (Automatic Voltage Regulator: AVR) and a capacitor voltage balancing control. First, the capacitor voltage averaging control regulates the average value of the capacitor voltages in the arm into the capacitor voltage command. On the other hand, the capacitor voltage balancing control corrects the unbalance among all capacitor voltages in the arm.

Besides, the PI controller in AVR outputs the positive-sequence component's command of the arm current. Therefore, the positive-sequence component of the arm current is regulated in order to maintain the capacitor voltages constant. On the other hand, the zero-sequence component of the arm current is applied in order to supply the output power to the DC micro-grid side. Note that the current controller in the proposed control is constructed by a P controller. Moreover, the control gain is defined as "K_{acr}".

3.1 Capacitor Voltage Averaging Control

The capacitor voltage averaging control regulates the average value of all capacitor voltages in the arm. Therefore, the average value of all capacitor voltages is required to be calculated in each arm. Each average value of the capacitor voltage is given by (5).

$$v_{cmk_ave} = \frac{2}{n} \sum_{x=1}^{n/2} v_{cmkx}, \quad m = A, B \quad k = r, s, t, \dots \dots \dots (5)$$

where v_{cmk_ave} is the average value of the capacitor voltage, m is the index which shows the upper side A or the lower side B, k is the index of each phase, m and k are matched in both sides of the equation.

The error between the capacitor voltage command and the average value of capacitor voltage in the arm is corrected by a PI controller. Therefore, the current command of the ACR is generated depending on the fluctuation of the average value of all capacitor voltages. However, the capacitor voltage includes the ripple voltage with same frequency as the grid frequency and the ripple voltage with twice frequency of the grid frequency when the cell capacitor is charged and discharged⁽²⁹⁾. Thus, the frequencies of the ripple voltages are 50 Hz and 100 Hz when the grid frequency is 50 Hz. The control may become unstable due to the ripple voltages because the ripple voltage becomes the disturbance to the capacitor voltage averaging control. Hence, in order to keep the stability of the control, the response angular frequency of the PI controller should be designed with the low bandwidth. On the other hand, when the high control response is required in the capacitor voltage averaging control, it is difficult to design the low bandwidth. Therefore, the band eliminated filter is applied in order to eliminate only the ripple voltage with the particular frequency such as 100 Hz. As a result, it is able to keep the stability and obtain the high control response of the proposed control.

3.2 Arm Current Control

In the MMC, the input AC current separately flows to the upper arm and the lower arm in each

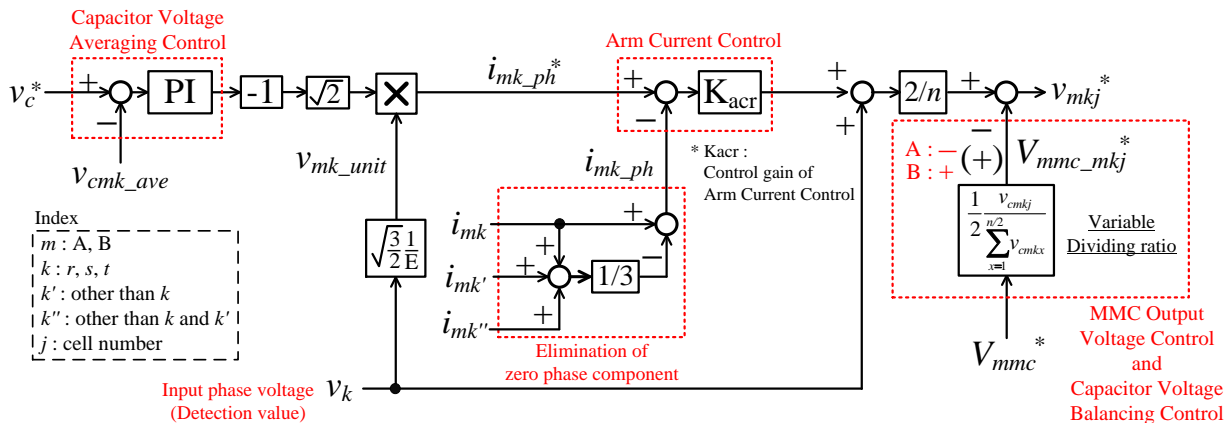


Fig. 3. Control block diagram of step-down rectifier which applies MMC. The proposed control is based on the control for general single phase power factor correction converters. Moreover, the proposed control is applied to each arm of the MMC in order to control each arm. Note that K_{acr} is the control gain of the arm current control, m is the index of the arm group A or B, k , k' or k'' is the index of the phase such as r , s and t , and j is the index of the cell number.

phase. Therefore, it is possible to control the input current by controlling the AC component of the arm current on each arm. The AC component of the arm current is defined as the positive-sequence component of the arm current. Moreover, the AC component of the arm current (the input current) flows to the MMC with the same cycle as that of the input voltage source. In addition, the output value of the PI controller of the AVR is given as the arm current command. Thus, the positive-sequence component is applied in order to control the average value of the all capacitor voltages. Additionally, in the general rectifier, the high input power factor is required. In the proposed control, the command of the positive-sequence component is multiplied by the sinusoidal wave of which phase is the same as one of the input phase voltage v_{k_unit} in order to be synchronized with the input phase voltage. Note that the amplitude of the sinusoidal wave v_{k_unit} is 1.0 in order to avoid the change of the current command. In addition, the coefficients in the latter part of the AVR is decided by the defined direction of the current in Fig. 1 and the calculation for the maximum value of the positive-sequence component.

On the other hand, each arm current also includes the DC component. The DC component of the arm current flows in order to supply the DC power into the micro-grid side. Additionally, the DC current shunts into the each leg of the MMC. Generally, the shunted DC current is constant and has same value among arms, when the output DC voltage of the MMC is equally divided among cells. In addition, the DC current is considered as the zero-sequence component because the DC current is temporally not changed and has no relationship to the cycle of the input voltage source.

The zero-sequence component becomes the disturbance to the arm current control (ACR) because the control objective of the arm current control is the positive-sequence component of the arm current. Thus, the zero-sequence component is eliminated from the actual detected current in order to apply only the positive-sequence component as feedback signal of the ACR.

Fig. 4 shows a schematic diagram of the arm current waveform. It is necessary to eliminate only the zero-sequence component from the actual arm current in order to apply only the positive-sequence component as the feedback signal of the ACR after the system detects all arm currents. In the proposed control method, the zero-sequence component is eliminated by adding and subtracting the detected arm current in each of the upper side and the lower side. In particular, the positive-sequence components are canceled each other and the total value of the zero-sequence components are extracted by the addition of the three arm currents in each of the upper side and the lower side. Moreover, the zero-sequence component of each arm current is calculated by dividing the total value of the zero-sequence components into three. Finally, only the positive-sequence component is extracted by subtracting each zero-sequence component from each detected arm current. As a result, the zero-sequence component is eliminated from each arm current. In addition, both the positive-sequence component and the zero-sequence component are equal on all arms when the output power of all cells is same and constant. Thus, the positive-sequence component is extracted without the unbalance on three arms of each side.

3.3 MMC Output Voltage Control The output DC voltage is supplied to the DC micro-grid side by applying the zero-sequence component. Thus, the command of the output DC voltage is added into the output value of the controller in the arm current control. The output DC voltage of the MMC is divided on each cell

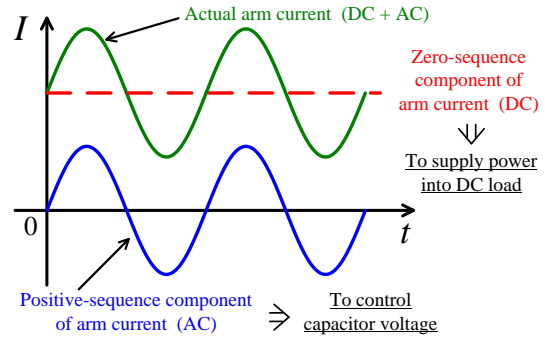


Fig. 4. Schematic diagram of current waveform on one arm. Each arm current includes the positive-sequence component (AC component) and the zero-sequence component (DC component). In order to control the capacitor voltage, it is necessary to eliminate the AC component from the arm current.

per leg. Hence, the output DC voltage of the cell is set V_{mmc}^*/n when the command of the output DC voltage is V_{mmc}^* and the number of cells per leg is n . Note that the output DC voltage of each cell is not completely same as V_{mmc}^*/n because the voltage dividing ratio of each cell is adjusted by the capacitor voltage balancing control. However, the error between the voltage dividing ratio which is adjusted by the capacitor voltage balancing control and V_{mmc}^*/n is sufficiently small. The detail is explained in the next section.

3.4 Capacitor Voltage Balancing Control The capacitor voltage averaging control is used to regulate the average value of all capacitor voltages. However, the unbalance voltage which occurs among capacitors in same arm cannot be suppressed by only the capacitor voltage averaging control, because the capacitor voltage averaging control corrects only the error between the voltage command and the average value of the capacitor voltages in the arm. So far, several methods in order to balance each capacitor voltage have been reported^{(8), (18)-(19)}. However, the design method of control parameters has not been reported. In addition, the positive-sequence component in order to keep the capacitor voltage flows to all cells which exist in one arm. Therefore, the positive-sequence component which flows to each cell is common. Thus, it is difficult to adjust the arm current in order to balance on each cell.

In contrast to the conventional control, in order to balance the capacitor voltage, in the proposed control, the output DC voltage of the cell is varied depending on the capacitor voltage. This control principle is given by (6).

$$V_{mmc_mkj}^* = A_{vd_mkj} V_{mmc}^*, \quad m = A, B \quad k = r, s, t, \dots \dots \dots (6)$$

where $V_{mmc_mkj}^*$ is the output DC voltage command of each cell, A_{vd_mkj} is the voltage dividing ratio of the output DC voltage on each cell, j is the index of the cell number, m , k and j are matched in both sides of (6).

The voltage dividing ratio of each cell A_{vd_mkj} is given by (7). The denominator of (7) shows the summation value of all capacitor voltages in each arm. The numerator of (7) shows the value of each capacitor voltage. From (7), A_{vd_mkj} is automatically adjusted depending on each capacitor voltage.

$$A_{vd_mkj} = \frac{1}{2} \frac{v_{cmkj}}{\sum_{x=1}^{n/2} v_{cmkx}}, \quad m = A, B \quad k = r, s, t, \dots \dots \dots (7)$$

For example, the voltage dividing ratio of each cell A_{vd_mkj} is set into a high value when its capacitor voltage is higher than the command of the capacitor voltage. Thus, the output power of its cell increases because the output voltage is increased by the high ratio of A_{vd_mkj} . Therefore, the capacitor is discharged. In contrast, A_{vd_mkj} is set into a low value when its capacitor voltage is lower than the command of the capacitor voltage. Thus, the output power of its cell decreases because the output voltage is decreased by the low ratio of A_{vd_mkj} . Hence, the capacitor is charged. Note that A_{vd_mkj} changes in steady state because each capacitor voltage v_{cmkj} and the sum value of all capacitor voltages in the denominator of (7) include the ripple voltage. On the other hand, the controller such as digital signal processor (DSP) or Field Programmable Gate Array (FPGA) calculates A_{vd_mkj} in each control period. Thus, the controller operates in order to correct the voltage errors among all capacitor voltages in each control period. In the ideal state without the ripple voltage, the output DC voltage of the cell is set V_{mmc}^*/n when the voltage values of all capacitors in the arm are same.

3.5 Unipolar Modulation for H-bridge Cell in MMC

In the proposed system, a unipolar modulation is applied for the operation of the H-bridge cell. In the general MMC, the chopper cell is applied. Therefore, the number of the voltage levels is determined by the number of cells. On the other hand, the output voltage of the H-bridge becomes the three-level voltage when the unipolar modulation is applied. Thus, the number of the voltage levels is increased compared to the chopper cell when the same number of cells is applied. Hence, the MMC with the H-bridge cell which the unipolar modulation is applied achieves the size reductions of the input filter circuit and the buffer inductors.

Fig. 5 shows the diagram of the unipolar modulation for the H-bridge cell (ex. v_{Arj}^*). The leg of the H-bridge cell is constructed by S_1 and S_2 . In contrast, the other leg is constructed by S_3 and S_4 . The switching patterns of S_1 and S_2 are determined by the voltage command v_{Arj}^* . Moreover, the switching patterns of S_3 and S_4 are determined by the inverted voltage command $-v_{Arj}^*$.

4. Capacitor Design

4.1 Capacitor Voltage The capacitor voltage command v_c^* is given by (1). Note that $V_{mmc_mkj}^*$ is slightly different among cells because the voltage dividing ratio of the output DC voltage A_{vd_mkj} is automatically adjusted depending on each capacitor voltage. However, the difference of $V_{mmc_mkj}^*$ among cells is ignored because the voltage margin of the capacitor is fully large compared to the difference of $V_{mmc_mkj}^*$ when the modulation index λ is set to 0.9 or less as with general power converters.

4.2 Capacitor Value The H-bridge cell has the same operation as the single-phase PFC converter in terms of the capacitor voltage control because both circuits regulate each capacitor voltage. Thus, the ripple voltage occurs when the H-bridge cell rectifies. The capacitor voltage includes the ripple voltage with same frequency as the grid frequency and the ripple voltage with twice frequency of the grid frequency⁽²⁹⁾. Generally, the ripple voltage affects the stability of the capacitor voltage control because the ripple voltage is the disturbance for the capacitor voltage control. Thus, the capacitance should be designed in order to reduce the effect by the ripple voltage for the capacitor voltage control. The problems due to the ripple voltage of the capacitors have been also discussed in the conventional single-phase PFC converters⁽³⁰⁾. Besides, the H-bridge cell of the MMC has same construction as that of the conventional single-phase PFC

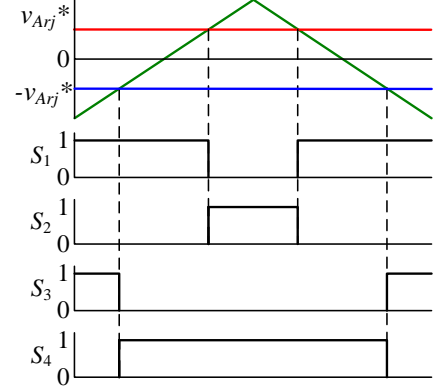


Fig. 5. Unipolar modulation for H-bridge cell (ex. v_{Arj}^*). The leg of the H-bridge cell is constructed by S_1 and S_2 . In contrast, the other leg is constructed by S_3 and S_4 . The switching patterns of S_1 and S_2 are determined by the voltage command v_{Arj}^* . Moreover, the switching patterns of S_3 and S_4 are determined by the inverted voltage command $-v_{Arj}^*$. From the above unipolar modulation, the output voltage of the H-bridge cell becomes three levels.

Table 2. Simulation conditions

Output power P_o	300 kW
Input line voltage rms E	6.6 kV
Input voltage frequency	50 Hz
Output voltage V_{mmc}	400 V
Number of cell per leg n	8
DC capacitor C	20000 μ F
Load R	0.54 Ω
Carrier frequency	1 kHz
Buffer inductor L_b	15 mH (%Z = 3.2%)

Table 3. Control parameters in simulation

Control gain of ACR K_{acr}	30
Proportional gain of AVR K_p	0.2
Integral time of AVR T_i	0.5 sec

converter. Therefore, it is possible to apply the design principle of the capacitance and the suppression method of the ripple voltage in the conventional single-phase PFC converter to the H-bridge cell without major modification. In the simulation of the circuit model which the input voltage is 6.6 kV and the power capacity is 300 kW, the capacitance is designed with the condition that the ripple voltage is 5% of the average value of the capacitor voltage.

5. Simulation Results

In this chapter, the fundamental operation of the step-down rectifier using the MMC is verified by simulation. Moreover, the stability for the mismatch of the circuit parameters is also evaluated.

Table 2 shows the simulation conditions. The proposed step-down rectifier which applies the MMC with 8 cells per leg converts commercial-frequency AC voltage of 6.6 kV into the DC voltage of 400 V.

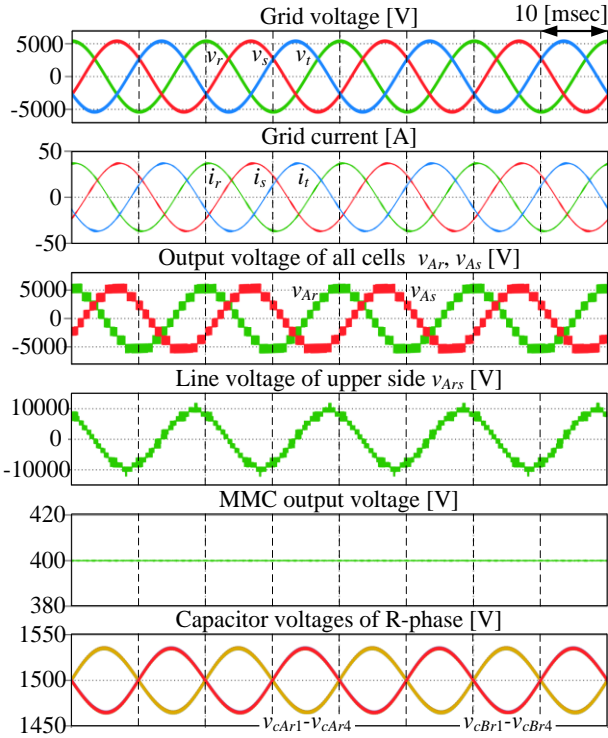


Fig. 6. Simulation result for operation of step-down rectifier which applies MMC. The proposed circuit achieves step-down rectification from line voltage of 6.6 kV to DC voltage of 400 V.

Table 3 shows the control parameters for the ACR and the AVR in the simulation. The main purpose of this paper is the verification of the MMC by the proposed control based on the single-phase PFC converter. Hence, the design of the control parameters for the single-phase PFC converter and the discussion about the optimization are omitted.

Fig. 6 shows the simulation results for the fundamental verification of the proposed step-down rectifier. At first, the output voltage of all cells in the upper side in R-phase or S-phase is nine-levels. In addition, the line voltage between R-phase and S-phase in upper side of the MMC is 17-levels. In the MMC with four H-bridge cells per arm, the arm voltage is nine-levels because the arm voltage is the summation of the output voltage of all cells in each arm. Thus, the step-down rectifier which applies the MMC achieves the size reduction of the buffer inductor compared to the H-bridge cell with the general bipolar modulation when the same number of cells is applied. Moreover, the step-down rectifier obtains the unity power factor because the phase difference of the input phase voltage and the input current is approximately 0. In addition, the total harmonic distortion (THD) of the input current is 0.1% or less when the normalized impedance %Z of each inductor is 3.2%.

On the other hand, the output voltage is maintained to 400 V. From the result, the MMC achieves step-down rectification from the line voltage of 6.6 kV to the DC voltage of 400 V.

Moreover, the all capacitor voltages are maintained constant. In addition, the maximum error between the voltage command and the simulation values is 0.1% or less. This result confirms the usability of the proposed capacitor voltage balancing control without the design of control parameters.

In addition, the stability is also evaluated for the parameter

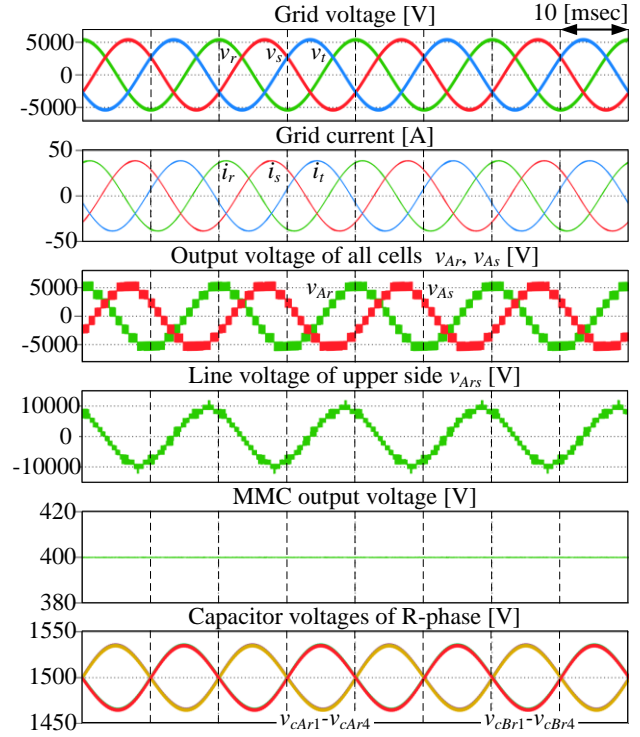


Fig. 7. Simulation results of proposed system when inductance is 30 mH (twice the value of the nominal value).

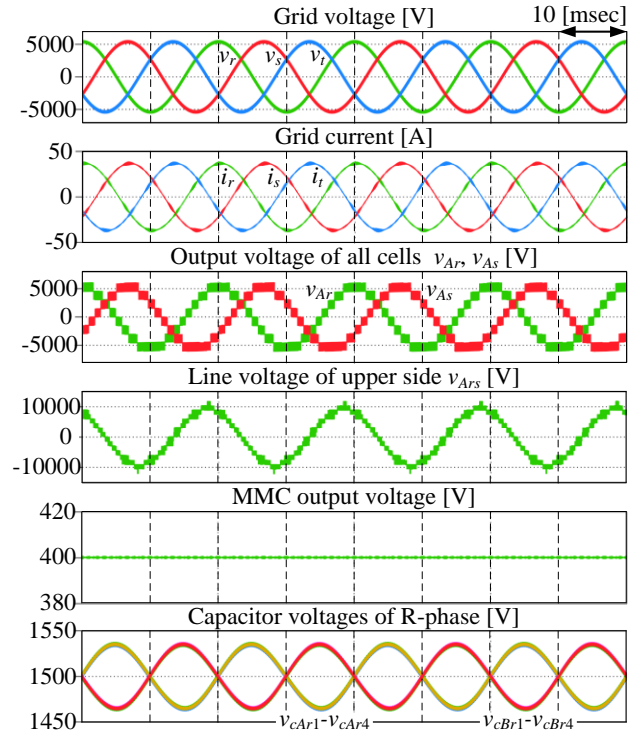


Fig. 8. Simulation results of proposed system when inductance is 7.5 mH (half the value of the nominal value).

mismatch of the inductance and the capacitance because the stable

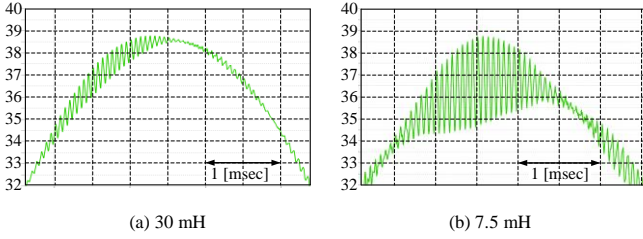


Fig. 9. Expanded waveform of the peak of inductor current when inductance is changed.

operation is required in the general converter even when the parameter mismatch occurs. In particular, the MMC can achieve the input current control, the MMC output voltage control and the capacitor voltage control. Thus, the waveforms when the parameter mismatch occurs are shown in order to evaluate the operation of the MMC.

From Fig. 7 to Fig. 11, the simulation results are shown in order to confirm the stability of the proposed control when circuit parameters change. In each simulation, the inductance and the capacitance are varied from 2.0 p.u. to 0.5 p.u. compared to the nominal values whose the inductance and the capacitance are 15 mH and 20000 μ F respectively.

Simulation results and waveforms when the inductance changes are as follows:

Fig. 7. Simulation result when the inductance is changed to 2.0 p.u. (30 mH);

Fig. 8. Simulation result when the inductance is changed to 0.5 p.u. (7.5 mH);

Fig. 9 (a). Expanded waveform of the peak of the inductor current when the inductance is 2.0 p.u. (30 mH); and

Fig. 9 (b). Expanded waveform of the peak of the inductor current when the inductance is 0.5 p.u. (7.5 mH).

From the comparison of two results when the inductance is varied, it is concluded that only the ripple of the inductor current changes. Furthermore, the effective value of the input current is slightly different because the input power factor changes by the inductance. However, there is no major difference such as the distortion of waveforms in both simulation results. As a conclusion, the proposed control is stable even when the inductance is mismatched.

After that, simulation results and waveforms when the capacitance is varied are as follows:

Fig. 10. Simulation result when the capacitance is changed to 2.0 p.u. (40000 μ F); and

Fig. 11. Simulation result when the capacitance is changed to 0.5 p.u. (10000 μ F).

From the comparison of the capacitor voltage waveforms (the lowest waveforms of each simulation results), the ripple of the capacitor voltage changes when the capacitance changes. Besides, the total harmonic distortion (THD) of the grid current in the MMC with the capacitance of 0.5 p.u. slightly becomes high because the output voltage of the cell is fluctuated by the ripple voltage. However, this THD of the grid current is still less than 1%. Additionally, there is no major difference in two simulation results. Thus, the proposed control is stable when the capacitance is mismatched.

In conclusion, the proposed system achieves the stable operation even when the circuit parameters of the inductance and the capacitance have the mismatches from 0.5p.u. to 2.0p.u..

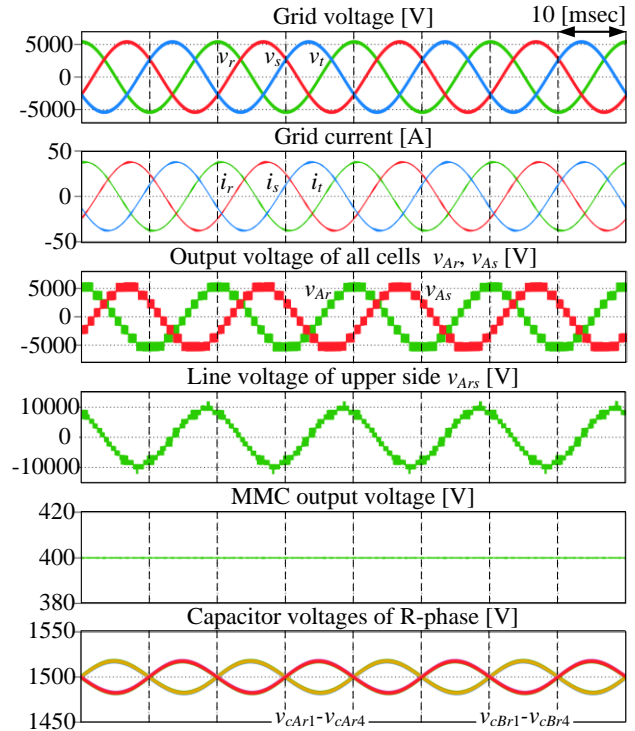


Fig. 10. Simulation results of proposed system when capacitance is 40000 μ F (twice the value of the nominal value).

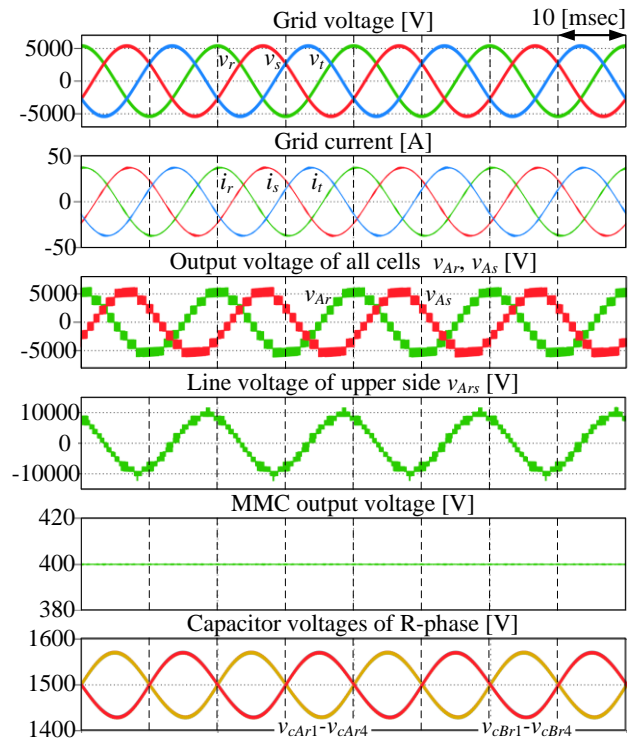


Fig. 11. Simulation results of proposed system when capacitance is 10000 μ F (half the value of the nominal value).

due to the DC component of the cell output voltage. However, the voltage fluctuation is small when the voltage level changes compared to that when applying the chopper cells and the H-bridge cells with bipolar modulation. Thus, the system achieves the size reduction of buffer inductors. Additionally, the frequency of the PWM pulse is decided by the equivalent frequency of the arm. In general, the equivalent frequency of the MMC is sufficiently high compared to the commercial frequency. Thus, the effect of the high frequency component is small even when the inductor is small because most of the high frequency is applied to the buffer inductor.

Fig. 15 shows the waveforms of all cell capacitor voltages which are connected to the R-phase leg. The cell capacitor voltage is controlled according to the capacitor voltage command v_c^* . As a result, the proposed step-down rectifier maintains the capacitor voltage of each H-bridge cell to the voltage command of 130 V. Therefore, the proposed rectifier also achieves the capacitor voltage control. In addition, the maximum voltage error between the voltage command of the cell capacitor and the measured voltage is 2% or less.

Fig. 16 shows the waveforms of the ripple voltages of all capacitors which are connected to the R-phase leg. In principle, each capacitor in the MMC has the ripple voltage whose frequency is based on the frequency of the input voltage⁽²⁹⁾. As a result, the waveforms of the ripple voltages with the low frequency are shown as same as the above discussion. Additionally, there is the error among capacitor voltages. However, as already discussed in Fig. 15, the voltage errors among all capacitors are very small compared to the average value of capacitor voltages.

Fig. 17 shows the relationship between the output power and the input power factor. The input power factor is over 0.95 when the output power is from approximately 0.2 p.u. to 1.0 p.u. (1000 W). Hence, the step-down rectifier which applies the MMC obtains the high power factor in the wide range of the power conversion.

Finally, from the above experimental results, the proposed step-down rectifier which applies the MMC achieves the input current control, the capacitor voltage control and step-down rectification at same time.

6.3 Verifications of Capacitor Voltage Control Fig. 18 shows the waveforms of the capacitor voltage when the command of the capacitor voltage changes in the step pattern of 0.23 p.u. (from 100 V to 130 V). The capacitor voltages converge to the command of the capacitor voltage. Additionally, the capacitor voltages are balanced.

Fig. 19 shows the waveform of the MMC output voltage when the command of the capacitor voltage changes in the step pattern of 0.23 p.u. (from 100 V to 130 V). All capacitor voltages converge to the command of the capacitor voltage. Furthermore, the MMC output voltage is maintained at constant even when the capacitor voltage changes.

Fig. 20 shows the waveforms of the capacitor voltage when the MMC output voltage changes in the step pattern of 0.27 p.u. (from 40 V to 60 V). All capacitor voltages converge to the command of the capacitor voltage and are maintained at same constant value. This result confirms the stable operation of the proposed capacitor voltage control even when the MMC output voltage is suddenly changed.

From above results, the proposed control maintains the capacitor voltage constant. Furthermore, the capacitor voltage balancing control is not necessary to design the control parameters and keep the balance of the capacitor voltage.

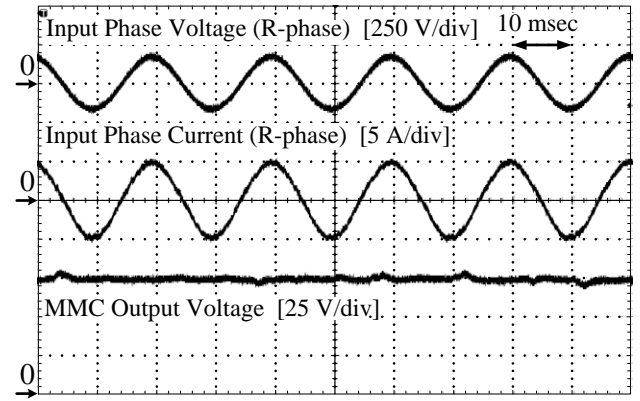


Fig. 13. Waveforms of input voltage, input current and output voltage. The unity power factor is obtained in the input stage. The THD of the input current is 3.5% when the %Z of the inductor is 6.1%.

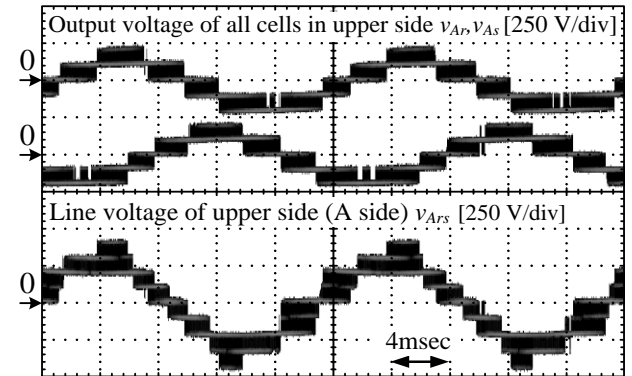


Fig. 14. Waveforms of arm voltage which is summation of output voltage of all cells in each arm and waveforms of line voltage between R-phase and S-phase in upper side. The arm voltage is five levels and the line voltage is nine levels.

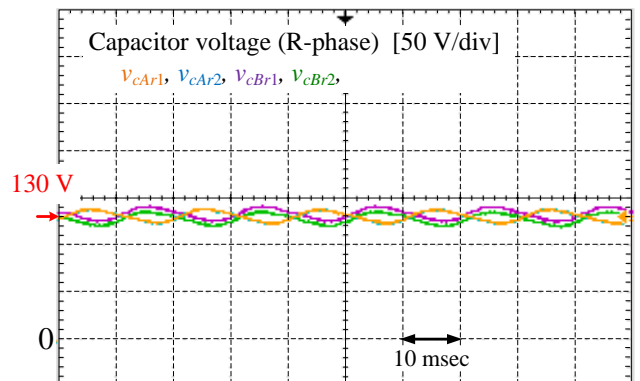


Fig. 15. Waveforms of all capacitor voltages in R-phase leg. The proposed system maintains the capacitor voltage of each H-bridge cell to the voltage command of 130 V. In addition, the maximum voltage error between the capacitor voltage command and the measured voltage is 2% or less.

7. Conclusion

In this paper, the fundamental verification of the control strategy for a step-down rectifier which applies the modular multilevel converter (MMC) was presented. The main part of the proposed control was based on the control method for a single-phase power factor correction converter (PFC converter) with the aim to apply many control techniques for the PFC converter to the MMC. Moreover, the proposed method of the capacitor voltage balancing control for all capacitor voltages did not require the design of the control parameters.

The fundamental operation was confirmed by the simulation. As a result, the proposed converter which applies the MMC achieved step-down rectification from the grid voltage of 6.6 kV to the DC voltage of 400 V. Moreover, the unity power factor was obtained in the input side of the MMC. The total harmonic distortion (THD) of the input current was approximately 0.1% when the nominalized impedance %Z of each inductor was 3.2%. Additionally, the step-down rectifier maintained all capacitor voltage at constant. Finally, the experimental results by the miniature model confirmed step-down rectification from the input voltage of 200 V into the output DC voltage of 75 V. Moreover, the proposed step-down rectifier maintained the capacitor voltage of each H-bridge cell to the voltage command of 130 V. The maximum error between the command of the capacitor voltage and the measured voltage was 2% or less.

Based on these results, it is confirmed that many control techniques for the single-phase PFC converter can be applied to the MMC. Moreover, it is not necessary to design many control parameters and consider the circuit models in order to clarify the control parameters. In addition, it is also expected that it is possible to propose new ideas and new points of view for a control method of the MMC by applying control technologies of the single-phase PFC converters. As a result, the discussion of the control method for the MMC will expand for the development of the MMC by new ideas and new points of view.

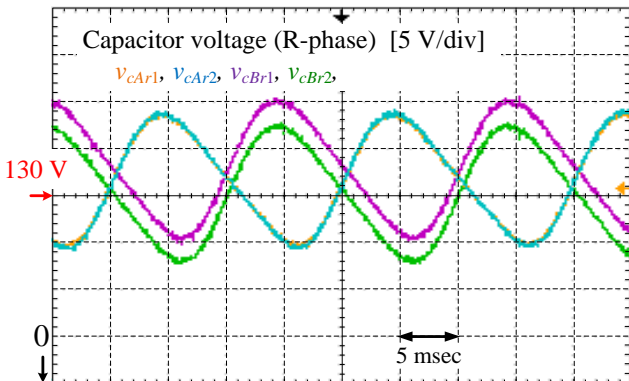


Fig. 16. Waveforms of ripple voltages of all capacitors which are connected to the R-phase leg. In principle, each capacitor in the MMC has the ripple voltage with the low frequency because the frequency of the ripple voltage is based on the frequency of the input voltage source.

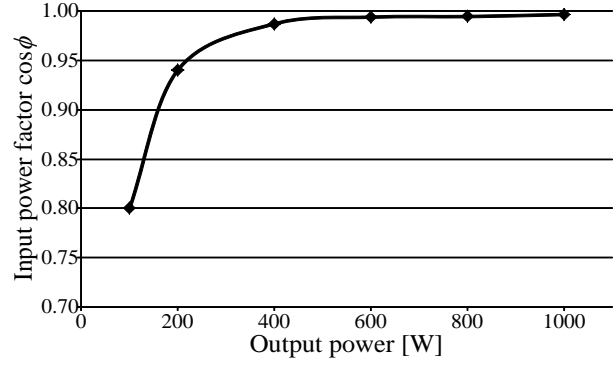


Fig. 17. Relationship between output power and input power factor. The input power factor is over 0.95 when the output power is from approximately 0.2 p.u. to 1.0 p.u. (1000 W). Thus, the system obtains the high power factor in the wide range of the power conversion.

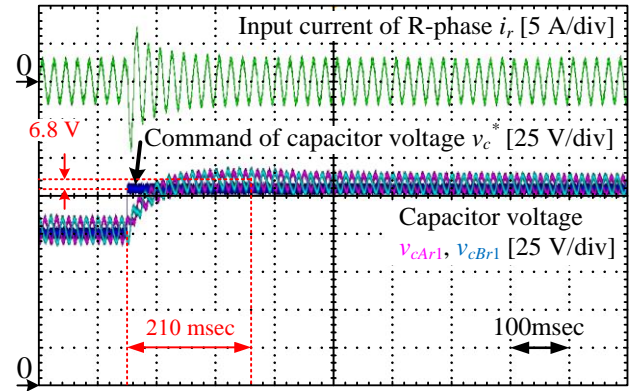


Fig. 18. Waveforms of capacitor voltage when command of capacitor voltage changes in step pattern of 0.23 p.u. (from 100 V to 130 V). All capacitor voltages converge to the command of the capacitor voltage after the capacitor voltage overshoots.

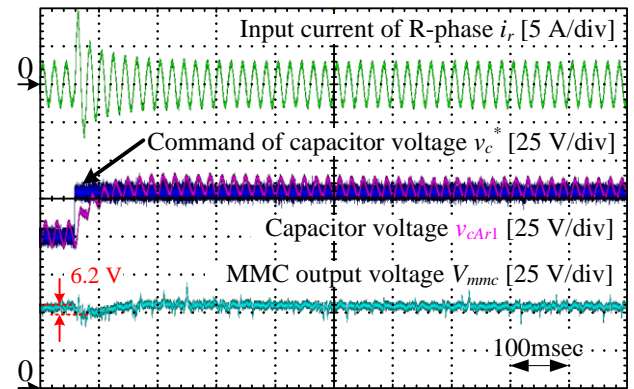


Fig. 19. Waveforms of MMC output voltage when command of capacitor voltage changes in step pattern of 0.23 p.u. (from 100 V to 130 V). The MMC output voltage is maintained at constant when the capacitor voltage changes.

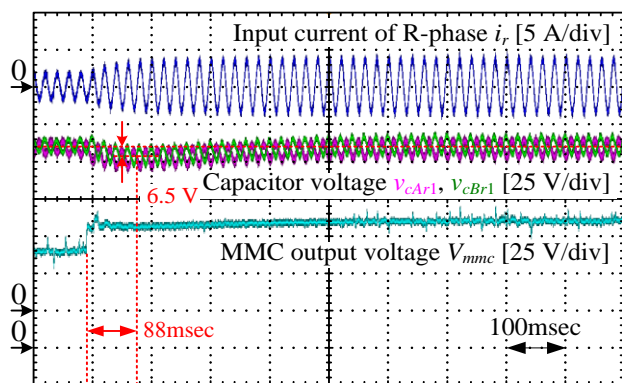
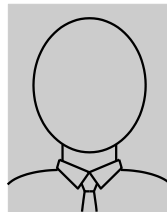


Fig. 20. Waveforms of capacitor voltage when MMC output voltage changes in step pattern of 0.27 p.u. (from 40 V to 60 V). All capacitor voltages are also balanced even when the MMC output voltage changes suddenly.

References

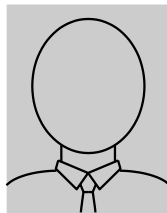
- (1) "Microgrids," *IEEE Power Energy Mag.*, vol. 6, no. 3, pp. 26-94, 2008.
- (2) H. Kakigano, Y. Miura, T. Ise, "Low-Voltage Bipolar-Type DC Microgrid for Super High Quality Distribution," *IEEE Trans. on Power Electronics*, vol. 25, no. 12, pp. 3066-3075, 2010.
- (3) D. Salomonsson, L. Söder, A. Sannino, "An Adaptive Control System for a DC Microgrid for Data Centers," *IEEE Trans. on Industry Applications*, vol. 44, no. 6, pp. 1910-1917, 2008.
- (4) D. Salomonsson, L. Söder, A. Sannino, "Protection of Low-Voltage DC Microgrids," *IEEE Trans. on Power Delivery*, vol. 24, no. 3, pp. 1045-1053, 2010.
- (5) M. Tabari, A. Yazdani, "Stability of a dc Distribution System for Power System Integration of Plug-In Hybrid Electric Vehicles," *IEEE Trans. on Smart Grid*, vol. 5, no. 5, pp. 2564-2573, 2014.
- (6) Y. Ito, Y. Zhongqing, H. Akagi, "DC microgrid based distribution power generation system," in *Proc. IEEE 4th Int. Power Electronics and Motion Control Conf. 2004. (IPEMC 2004)*, vol. 3, pp. 1740-1745, 2004.
- (7) M. Glinka, R. Marquardt, "A New AC/AC Multilevel Converter family," *IEEE Trans. on Industrial Electronics*, vol. 52, no. 3, pp. 662-669, 2005.
- (8) M. Hagiwara, H. Akagi, "Control and Experiment of Pulsewidth-Modulated Modular Multilevel Converters," *IEEE Trans. on Power Electronics*, vol. 24, no. 7, pp. 1737-1746, 2009.
- (9) H. Akagi, "Classification, Terminology, and Application of the Modular Multilevel Cascade Converter (MMCC)," *IEEE Trans. on Power Electronics*, vol. 26, no. 11, pp. 3119-3130, 2011.
- (10) M. Vasiladiotis, S. Kenzelmann, N. Cherix and A. Rufer, "Power and DC Link Voltage Control Considerations for Indirect AC/AC Modular Multilevel Converters", *Power Electronics and Applications 2011. (EPE 2011)*, Proceedings of the 2011-14th European Conference, 2011.
- (11) J. Shi, W. Gou, H. Yuan T. Zhao, A. Q. Huang, "Research on Voltage and Power Balance Control for Cascaded Modular Solid-State Transformer", *IEEE Trans. on Power Electronics*, vol. 26, no. 4, pp. 1154-1166, 2011.
- (12) K. Ilves, L. Harnefors, S. Norrga, H-P. Nee, "Analysis and Operation of Modular Multilevel Converters With Phase-Shifted Carrier PWM," *IEEE Trans. on Power Electronics*, vol. 30, no. 1, pp. 268-283, 2015.
- (13) S. Debnath, M. Saeedifard, "A New Hybrid Modular Multilevel Converter for Grid Connection of Large Wind Turbines," *IEEE Trans. on Sustainable Energy*, vol. 4, no. 4, pp. 1051-1064, 2013.
- (14) N. Thitichaiworakorn, M. Hagiwara, and H. Akagi, "Experimental Verification of a Modular Multilevel Cascade Inverter Based on Double-Star Bridge Cells," *IEEE Trans. on Industry applications*, vol. 50, no. 1, pp. 509-519, 2014.
- (15) M. Vasiladiotis, A. Rufer, "Analysis and Control of Modular Multilevel Converters with Integrated Battery Energy Storage," *IEEE Trans. on Power Electronics*, vol. 30, no. 1, pp. 509-519, 2015.
- (16) G. Minyuan and X. Zheng, "Modeling and Control of a Modular Multilevel Converter-Based HVDC System Under Unbalanced Grid Conditions," *IEEE Trans. on Power Electronics*, vol. 27, pp. 4858-4867, 2012.
- (17) F. Deng, Z. Chen, "Voltage-Balancing Method for Modular Multilevel Converters Switched at Grid Frequency," *IEEE Trans. on Industrial Electronics*, vol. 62, no. 7, pp. 4158-4169, 2015.
- (18) A. Hassanpoor, L. Ängquist, S. Norrga, K. Ilves, H-P. Nee, "Tolerance Band Modulation Methods for Modular Multilevel Converters," *IEEE Trans. on Power Electronics*, vol. 30, no. 1, pp. 311-326, 2015.
- (19) D. Karagiannis, E. Mendes, A. Astolfi, R. Ortega, "An Experiment Comparison of Several PWM Controllers for a Single-phase AC-DC Converter," *IEEE Trans. on Control Systems Technology*, vol. 11, no. 6, pp. 311-326, 2003.
- (20) B-R. Lin, H-H. Lu, S-C. Tsay, "Control Technique for High Power Factor Multilevel Rectifier," *IEEE Trans. on Aerospace and Electronic Systems*, vol. 37, no. 1, pp. 226-240, 2001.
- (21) G. Escobar, D. Chevreau, R. Ortega, E. Mendes "An Adaptive Passivity-Based Controller for a Unity Power Factor Rectifier," *IEEE Trans. on Control Systems Technology*, vol. 9, no. 4, pp. 637-644, 2001.
- (22) J-C. Crebier, J-P. Ferrieux, "PFC Full Bridge Rectifiers EMI Modeling and Analysis - Common Mode Disturbance Reduction," *IEEE Trans. on Power Electronics*, vol. 19, no. 2, pp. 378-387, 2004.
- (23) H. Akagi, T. Yamagishi, N. M. L. Tan, S. Kinouchi, Y. Miyazaki, M. Koyama, "Power-Loss Breakdown of a 750-V 100-kW 20-kHz Bidirectional Isolated DC-DC Converter Using SiC-MOSFET/SBD Dual Modules," *IEEE Trans. on Industry Applications*, vol. 51, no. 1, pp. 420-428, 2015.
- (24) B. Zhao, Q. Song, W. Liu, Y. Sun, "Overview of Dual-Active-Bridge Isolated Bidirectional DC-DC Converter for High-Frequency-Link Power-Conversion System," *IEEE Trans. on Power Electronics*, vol. 29, no. 8, pp. 4091-4106, 2014.
- (25) J. W. Kolar, G. Ortiz, "Solid-State-Transformers: Key Components of Future Traction and Smart Grid Systems," Proceedings of the International Power Electronics Conference - ECCE Asia (IPEC 2014), 2014.
- (26) [Online] <https://www.infineon.com>
- (27) [Online] <http://www.hitachi-power-semiconductor-device.co.jp>
- (28) [Online] <https://library.e.abb.com>
- (29) T. Nakanishi, J. Itoh : "Capacitor Volume Evaluation based on Ripple Current in Modular Multilevel Converter", 9th International Conference on Power Electronics, No. WeA1-5, 2015.
- (30) Y. Ohnuma, J. Itoh, "A Novel Single-Phase Buck PFC AC-DC Converter With Power Decoupling Capability Using an Active Buffer," *IEEE Trans. on Industrial Application*, vol. 50, no. 3, pp. 1905-1914, 2014.

Toshiki Nakanishi



(Student member) received the B.S. degrees in electrical, electronics and information engineering from Nara National College of Technology (NNCT), in 2011. He received master degrees in Nagaoka University of Technology (NUT) in 2014. And he has been in doctoral course of NUT. He is the student member of IEEJ and IEEE. His main research interests include multilevel converters.

Jun-ichi Itoh



(Senior Member) received his M.S. and PhD degrees in electrical and electronic systems engineering from Nagaoka University of Technology, Niigata, Japan in 1996 and 2000, respectively. From 1996 to 2004, he was with Fuji Electric Corporate Research and Development Ltd., Tokyo, Japan. Since 2004, He has been with Nagaoka University of Technology as an associate professor. He received the IEEJ Academic Promotion Award (IEEJ Technical Development Award) in 2007 and the Isao Takahashi Power Electronics Award in 2010. His research interests include matrix converters, DC/DC converters, power factor correction techniques and motor drives. He is a senior member of the Institute of Electrical Engineers of Japan and the Society of Automotive Engineers of Japan.